21st International Conference on
Harmonisation within Atmospheric Dispersion Modelling for Regulatory Purposes
27-30 September 2022, Aveiro, Portugal

# NEW INSIGHT ON 3D MODELLING OF THE DISPERSION OF GASES RELEASED FROM AN INDUSTRIAL FACILITY IN A COMPLEX ENVIRONMENT

*Patrick Armand[1] and Christophe Duchenne[1]*

[1]CEA, DAM, DIF, F-91297 Arpajon, France

**Abstract:** Routine operation of industrial plants as possible accidents that cannot be ruled out result in releases of gases or particles into the air. The accurate simulation of the space and time distribution of these emissions is crucial to assess their harmlessness to health and the compliance with the environmental regulation in normal conditions and to estimate any potential health impact in adverse conditions. Most of the industrial sites encompass built-up areas and are located in complex environments characterized by a rugged terrain and a heterogeneous land use. As the Gaussian-type models are definitely not adapted to these configurations, this paper dedicates to exemplifying the use of a 3D modelling system in the case of authorized gaseous releases from the plants of a research center. The main steps of the study consist in creating the 3D numerical mock-up of the site under consideration and perfoming twin experiments of the hourly flow and dispersion for the whole year 2018. The wind and concentration fields are strongly influenced by the topography and land use over the whole terrain and, locally, by the buildings. The comparison between the simulated concentrations and measurements at some monitoring points highligths some discrepancies for which explanations are provided. While our results need further analysis, they illustrate the interest of 3D modelling in the field of impact assessment.

***Key words:*** *3D multi-scale modelling, atmospheric flow and dispersion, impact assessment.*

## INTRODUCTION

Most industrial facilities release gaseous or particulate, chemical or radioactive materials in the atmosphere. Authorized and controlled emissions must obviously be totally harmless for the population and their impact on the environment must be as limited as possible and comply with the regulation. Furthermore, the health consequences of potential accidental emissions must be assessed in advance in order to anticipate adapted counter-measures. Whatever the type of release, the facility operators should know and be able to determine the space and time distribution of the materials, which their plants are likely to release in the atmosphere.

Even today, Gaussian models are extensively used to assess the impact of atmospheric releases on health and the environment, at least for regulatory purpose. Yet, the assumptions underlying these models, namely a flat unobstructed terrain and a uniform wind field are far from being verified on real sites and in real life. While some Gaussian models were upgraded to take account of isolated buildings or specific configurations like street canyons, they cannot encompass the complexity and diversity of most industrial sites. Above all, simplistic models may be inappropriate for the proper and rigorous impact assessment of industrial plants, one major conclusion of the COST Action ES 1006 (Armand *et al.*, 2015; Baumann Stanzer *et al.*, 2015).

Conversely, the 3D models provide realistic results, thus a better insight into the consequences of normal or accidental atmospheric releases (Armand and Duchenne, 2019a, 2019b; Armand et al., 2021). While not restrained by oversimplifying hypotheses, these models benefit from thorough development and validation, and from increasingly affordable powerful computational resources. In this context, we have engaged for more than ten years in the development of a generic and flexible high resolution modelling system capable of downscaling weather forecast from meso-scale to local scale and simulating the transport, dispersion and deposition of gases or particles released into the air in routine operation or in the event of an accident.

Local scale simulations are carried out with PMSS, which is the parallel version of Micro-SWIFT-SPRAY, developed as a quick solution of the 3D flow and dispersion in built-up environments. PMSS combines the Micro-SWIFT mass-consistent diagnostic flow model and Micro-SPRAY Lagrangian particle dispersion model (Tinarelli et al., 2013). The major features of PMSS are to deal with nested domains and to explicitly account for the effects of the obstacles on the flow and dispersion. The parallelization of PMSS has proven to be efficient in very large and highly resolved computational domains (Oldrini, Armand *et al.*, 2017, 2019, 2021a, 2021b). A great attention has been paid to PMSS validation against numerous experimental trials in wind tunnel and at full scale (Trini Castelli et al., 2016, 2018; Oldrini and Armand, 2019).

This short paper is the continuation of two previous papers (Armand and Duchenne, 2021a and 2021b) that present the application of our modelling system to evaluate the incidence of routine operation conditions at a research center. In the absence of total containment, some facilities release authorized amounts of gases into the atmosphere. The site under consideration has complex features. Indeed, it has a quite large number of buildings and it is located on a plateau surrounded by a rugged terrain. Our 3D modelling system is used to simulate the flow and the distribution of the gases for the whole 2018 year in order to eventually check that the activities of the center do not have any consequences on health and the environment.

In the paper, we first present the flow results interpreted according to the characteristics of the environment such as the hilly terrain and presence of forested areas. Then, we comment on the dispersion results, which show a variably satisfactory agreement between the calculated and measured concentrations at the different monitoring points. As a conclusion, tentative explanations of the discrepancies between computations and measurements are proposed. Details abut the meteorological characterization of the site and the dispersion computations can also be found in our previous papers (Armand and Duchenne, 2021a and 2021b).

## METEOROLOGICAL DATA AND FLOW SIMULATIONS

### Meteorological study

First, we carried out a meteorological study with the available data for the year 2018 chosen as an example. On one hand, **Figure 1** shows the wind rose built using the data of the meteorological mast set up on the center measuring the wind speed and direction at 10 m and the air temperature at 2 m above the ground. On the other hand, AROME hourly data projected on a regular mesh with a resolution of 0.025° (*i.e.* 2.7 km x 1.9 km in the SN and WE directions) were compiled to establish wind roses in 5 velocity and 36 direction classes (like for the wind rose of the mast). **Figure 2** shows that the AROME wind roses at the 45 points of the AROME grid over the simulation domain of 13 km x 14 km centered on the site. While the area under consideration is quite small, AROME wind roses present disparities due to orographic and land use effects. Furthermore, AROME data extracted at the coordinates of the mast are very close to the wind data measured on the mast. Thus, we decided to use AROME as input data of Micro-SWIFT flow model in PMSS.

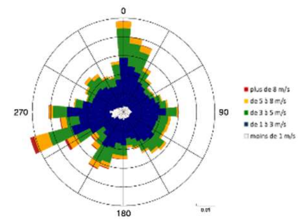


**Figure 1.** Wind rose in 2018 at a height of 10 m built from data measured on the meteorological mast.

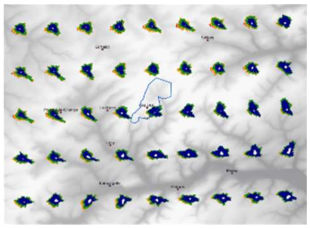

**Figure 2.** Wind roses in 2018 at a height of 10 m built from AROME data (Météo France).

### Micro-scale meteorological simulations

The resolution of meso-scale flow data may be insufficient to account for narrow valleys around the site with a width of 1 km or less and is not suitable for simulations around and in-between buildings. Therefore, AROME hourly data (wind, temperature…) were downscaled for the whole year 2018 using PMSS.

**Figure 3** and **Table 1** give features of PMSS computational domains. The largest domain has a resolution of 20 m and is divided into nine tiles so that the memory capacity of the computer nodes is not exceeded. Six local domains have a resolution of 2 m and cover the upper part and the lower part of the center, as well as four villages surrounding the center where atmospheric sampling devices are installed and in operation.

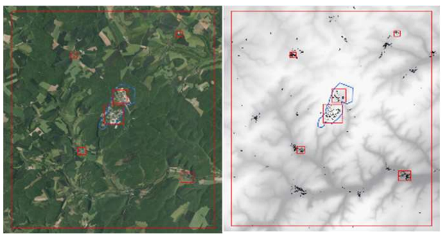

**Figure 3.** View of the PMSS nested simulation domains.

**Table 1.** Features of PMSS computational grids.

| Domain | Resolution (in m) | Dimensions (in km x km) | Number of nodes | Division into tiles |
|---|---|---|---|---|
| Large one | 20 | 12.98 x 13.98 | 650 x 700 | Yes (9 tiles) |
| Center upper | 2 | 1.24 x 1.22 | 621 x 611 | Yes (4 tiles) |
| Center lower | 2 | 0.92 x 0.86 | 461 x 431 | No |
| Village L | 2 | 0.50 x 0.45 | 251 x 226 | No |
| Village M | 2 | 0.80 x 0.65 | 401 x 326 | No |
| Village E | 2 | 0.40 x 0.35 | 201 x 176 | No |
| Village S | 2 | 0.40 x 0.35 | 201 x 176 | No |

### Results of micro-scale flow calculations

**Figure 4** shows the wind field over the large domain at a height of 10 m on 1 Nov. 2018 at 9:00. **Figure 5** shows the wind field over the upper part of the center at a height 2 m (same timeframe). While the buildings influence the wind speed and direction, their wakes interact only weakly as they are distant from each other. **Figure 6** shows the wind field over village E domain at a height of 2 m (same timeframe). Old construction houses, close to each other, lead to a complex pattern with wakes interacting inside the streets of the village.

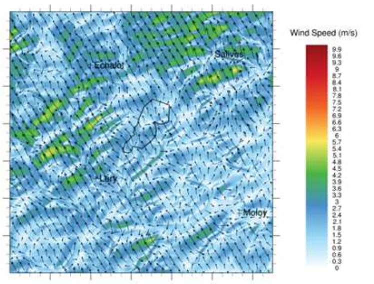

**Figure 4.** Wind field at 10 m on the regional domain on 1 Nov. 2018 at 9:00.

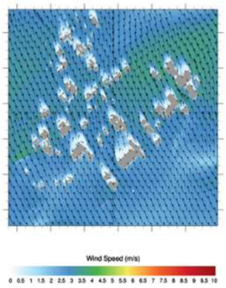

**Figure 5.** Wind field at 2 m on the upper part of the center on 1 Nov.2018 at 9:00.

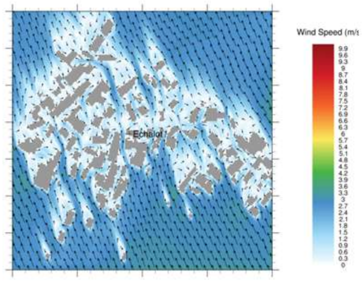

**Figure 6.** Wind field at 2 m on the village E domain on 1 Nov. 2018 at 9:00.

## DISPERSION SIMULATIONS

Micro-SPRAY simulations were carried out in order to evaluate the spatio-temporal repartition of the gases emitted through the stacks of some facilities of the research center. Of course, these releases are authorized and strictly controlled. Depending on the plants, the releases are unequal in amplitude and time distribution, both daily and seasonally, in particular due to different activities performed. High frequency measurements show that the actual timing of the releases is complex and has both a background and a number of peaks.

In total, eight emission sources were represented by numerical particle numbers proportional to the releases, corresponding to several hundred billion particles for the whole of 2018. The dispersion computations were linked in chronological order (*i.e.* the particle plume at the end of a calculation initiates the following one). The dry deposition on the ground and washing by the rain of the gaseous emissions were taken into account. Finally, atmospheric concentrations were averaged and stored on an hourly basis throughout 2018.

Dispersion simulations were performed without the buildings in the 20 m resolution domain, and with the buildings considering the 20 m domain and the 6 domains of 2 m resolution divided (*cf.* **Table 1**). Buildings were accounted for in the villages where sampling stations are set up in order to study their possible effect on the concentration measurements. Air intake on the roof of the sampling stations is located at the height of 3 m, at which the concentrations results are shown.

### Distribution of the releases without accounting for the built-up environment

**Figure 7** shows the spatial distribution of the atmospheric concentration on 1 Nov. 2018 averaged between 8:00 and 9:00 and between 18:00 and 19:00 at a height of 3 m above the ground, following the releases of all facilities. The plumes are relatively straight, even when the wind is blowing at low speed around 19:00. The influence of the relief is visible in the valleys perpendicular to the axes of progression of the plumes. The low ground concentrations indicate that the plume passes over the valley without descending the slopes. **Figure 8** shows the annual average concentration computed for all releases for the year 2018. The maximum concentration is within the center. Outside, the concentration is very low everywhere. It appears clearly that the repartition near the ground is influenced by the relief and land use. The concentrations evaluated inside the valleys, even the small ones, are much lower than the concentrations on the neighboring plateaus.

### Distribution of the releases accounting for the built-up environment

**Figure 9** shows the spatial distribution of the atmospheric concentration on 1 Nov. 2018 averaged between 8:00 and 9:00 and between 18:00 and 19:00, near the ground. The plumes are similar to those in **Figure 7**. Thus, the buildings' influence on the repartition of the releases is not significant outside of the center limits. **Figure 10** shows the average concentration field on the village S domain on 1 Nov. 2018 between 18:00 and 19:00. Despite a pixilation effect inherent to the Lagrangian dispersion model and the cells of different volumes in the nested domains, low concentrations are observed in the wakes of the buildings. Consistently, the wakes extend downstream from the 2 m resolution domain into the 20 m resolution domain.

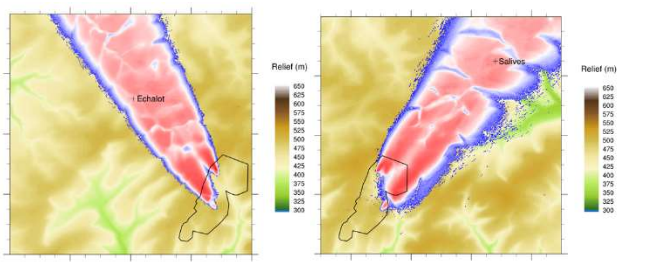


**Figure 7.** Concentration fields at 3 m on 1 Nov. 2018 at 9:00 and 19:00, following the releases from all the installations (without the buildings).

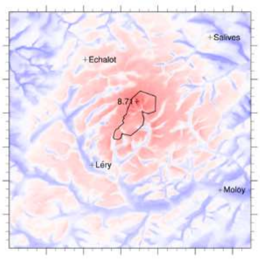


**Figure 8.** Annual average concentration at 3 m for the releases of the year 2018.

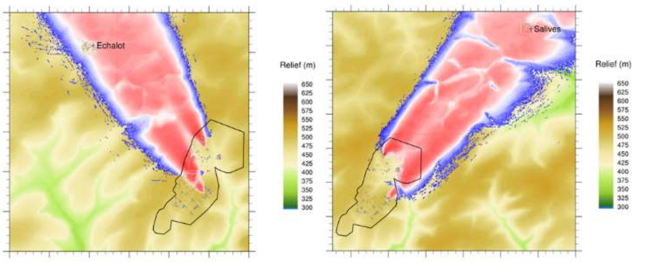


**Figure 9.** Concentration fields at a 3 m on 1 Nov. 2018 at 9:00 and 19:00, following the releases from all the installations (buildings accounted for).

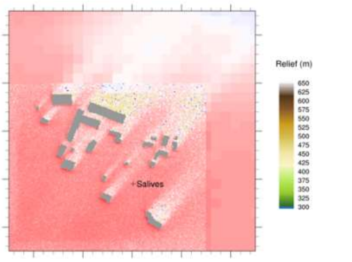


**Figure 10.** Zoom on the village S of the concentration on 1 Nov. 2018 at 19:00.

**Vertical cross sections of plumes**

**Figure 11** and **Figure 12** show vertical sections of the turbulent kinetic energy on the left and concentration on the right simulated by PMSS. The thin black line is the mixing height estimated by the AROME model. The former figure corresponds to the stable meteorological situation on 4 Nov. 2018 at 18:00. The released gas is distributed relatively evenly in a layer less than 200 meters high, between the ground and the mixing height. The concentration decreases, then increases from east to west. This is because the followed plume has its axis not exactly in the section plane and merges with other plumes in the western part of the section. The latter figure corresponds to a slightly unstable meteorological situation on 11 May 2018 at 9:00. After one kilometer, the released gas mixes efficiently over the height of around 600 meters of the mixing layer. These situations exemplify that the plume vertical diffusion is consistent with the atmospheric stability.

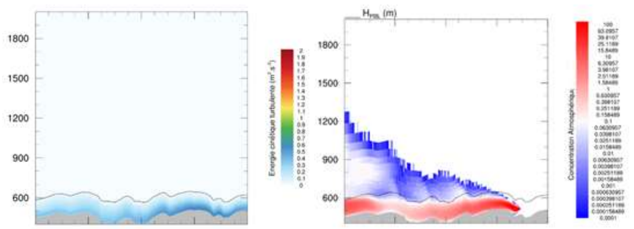


**Figure 11.** West-east vertical sections of the turbulent kinetic energy and concentration fields on 4 Nov. 2018 at 18:00.

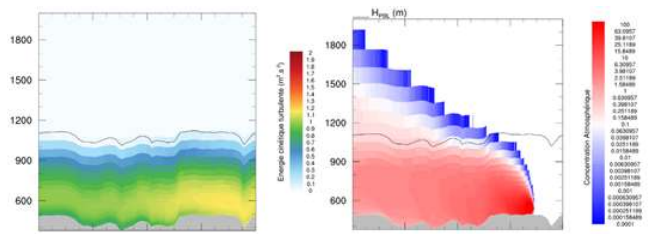


**Figure 12.** West-east vertical sections of the turbulent kinetic energy and concentration fields on 11 May 2018 at 09:00.

**Comparison of the computations to environmental measurements**

Villages around the center are equipped with continuous sampling stations providing weekly measurements of the local atmospheric volume concentrations. These measurements as the concentrations computed over the same time intervals show a strong spatial variability even by averaging the concentrations over a week.

**Figure 13** shows, by way of example, the time series of the weekly concentration measured at the village S station (blue curve) and computed by Micro-SPRAY (red and green curves) at the same coordinates and at 3 m above the ground. The shaded areas indicate the uncertainty associated with the measurement. When the measurement is below the detection limit (DL), the shaded area extends from 0 to the value of the DL. Measurements below the LD are associated with zero or very low calculated concentrations. In the case of measurements above the LD, the simulated activities are most often outside the confidence interval. When comparing the numerical results with the measurements, it can be observed that the dynamics of the signal is globally correct but the simulated concentrations are noticeably lower than the measured concentrations. This is visible in the same way at the other three sampling stations.

Such discrepancies between calculations and measurements are unusual in the implementation of PMSS, which has given very satisfactory results in many validation test cases and respects the criteria of Hanna and Chang (2012). In order to check our results, an alternative series of hourly dispersion simulations (green curve) in the period between May and December 2018 was run changing some modelling options. While the characteristics of the atmosphere and turbulence were evaluated directly by Micro-SWIFT in the first computations (red curve), we estimated them from the AROME data in the second series of computations (green curve). The Monin-Obukhov length as the standard deviations of the fluctuating velocities and the Lagrangian time scales were computed in an external module using AROME turbulent kinetic energy data. Then, these fields were interpolated by Micro-SWIFT before being input to Micro-SPRAY. As a result, the concentrations are comparable whether they are computed by Micro-SWIFT or derived from AROME.

**Figure 14** shows the time series of the weekly concentration measured at the village S station (blue curve) and computed by Micro-SPRAY (red curve) over the last eight months of the year 2018. In addition, Micro-SPRAY results are given in the 26 adjacent grid cells around the coordinates of the station. While there is a low horizontal variability, the concentrations generally increases with the elevation, up to a factor of two, or decreases at some times. However, the numerical results remain lower than the measurements.

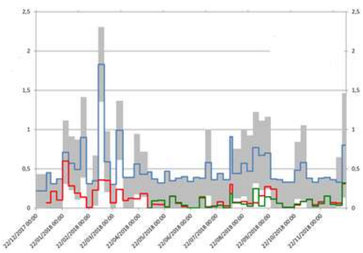

**Figure 13.** Comparison of measurements at village S with the concentrations calculated by Micro-SPRAY in two different ways.

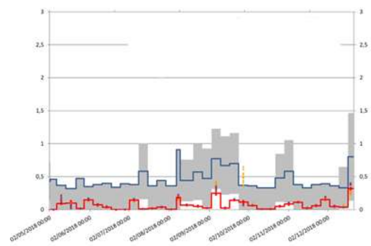

**Figure 14.** Comparison of measurements at village S with the concentrations calculated by Micro-SPRAY at 26 grid points around the measurement point.

While the previous figure shows the concentration variations in the limited vicinity of a measuring station, **Figure 15** and **Figure 16** illustrate the concentration sensitivity to the location in the simulation domain. More precisely, these figures present the zones (in blue) where the average simulated concentrations at a height of 3 m are greater than the measurement on the station and for the weekly period under consideration (taking account of the measurement uncertainty). While the concentrations evaluated by Micro-SPRAY are lower than the measured ones at the position of the station, they are comparable to the measurements at a distance of only 200 m in the chosen cases where the sampling stations are located at the bottom of valleys.

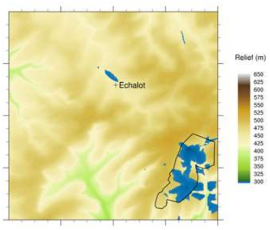


**Figure 15.** Zones in blue where the average simulated concentration between 3 and 10 Sept. 2018 is greater than the measured concentration at village E.

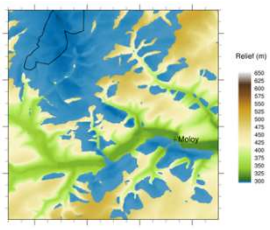


**Figure 16.** Zones in blue where the average simulated concentration between 4 and 11 June 2018 is greater than the measured concentration at village M.

## CONCLUSIONS

This short paper sums up the 3D simulations of the airflow and dispersion of gases emitted by the facilities at a research center comprising several buildings and located on a rugged terrain. Computations are carried out on an hourly basis throughout 2018 using a 3D digital mock-up and PMSS modelling system, explicitly accounting for the topography, the land use and the buildings on the site and in neighboring villages where environmental monitoring stations are set up. There is a principal simulation domain whose dimensions are 13 x 14 km and resolution is 20 m 2 m with nested domains of resolution 2 m encompassing the buildings.

PMSS flow and dispersion simulations bring out several interesting points, some of which are listed here:

- Wind roses derived from AROME or Micro-SWIFT meteorological data turn out to be different even for adjacent grid points due to the contrasted relief, land use, and presence of built up areas.
- AROME or Micro-SWIFT results compare very well with the wind measurements at the mast.
- Hourly as average annual concentrations computed with Micro-SPRAY reveal orographic effects on the large domain and, more locally, areas in the buildings' wakes sheltered from the plumes.
- Turbulent fields input to Micro-SPRAY were either evaluated by Micro-SWIFT or inferred from the AROME data. Whatever the model, the concentrations simulated over weekly periods at the monitoring stations tend to underestimate the measurements. Nowadays, the preferred explanation is related to the source terms, which are known on average over one week, whereas high-resolution measurements show peaks of one hour or less up to 100 times higher than the background releases. Thus, detections above the DL are rare events combining enough high amplitude emissions from one or several sources synchronized with meteorological conditions heading the releases to the measurement stations. We also showed that the concentration field has strong gradients due to the narrow plumes above the uneven terrain. It is thus likely that simulated plumes will miss stations.
- Notwithstanding future work aimed at solving the above-mentioned discrepancies, the hourly, as the annual concentrations are very low, which demonstrates a weak marking of the environment.

Eventually, the 3D simulations reveal the significant influence of the relief, land use and buildings on the flow and dispersion of releases into the atmosphere. Therefore, 3D models should be leveraged in order to more realistically and reliably evaluate the space and time repartition of gases or particles emitted in the air and more safely and convincingly assess their impact on health and the environment.

## REFERENCES


Armand, P. et al., 2015: Best Practice Guidelines for the use of Atmospheric Dispersion Models in Emergency Response Tools at local-scale in case of hazmat releases into the air. COST Action ES1006.

Armand, P. and C. Duchenne, 2021b: 3D multi-scale weather and dispersion models applied to assess the impact of industrial plants on human health and the environment. Proc. 38th Int. Technical Meeting on Air Pollution Modelling and its Application, ITM 2021, Barcelone, Spain, 18-22 Oct. 2021.

Armand, P. and C. Duchenne, 2021a: A new methodology based on 3D multi-scale modelling to assess the impact on health and the environment of industrial facilities. Proc. 20th Int. Conf. on Harmonisation within Atmospheric Dispersion Modelling for Regulatory Purposes, Tartu, Estonia, 14-18 June 2021.

Armand, P. and C. Duchenne, 2019b: Urgency management of adverse atmospheric releases with a forefront multi-scale high resolution modelling and decision-support system. Proc. 37th Int. Technical Meeting on Air Pollution Modelling and its Application, Hamburg, Germany, 23-27 Sept. 2019.

Armand, P. and C. Duchenne, 2019a: A multi-scale modelling system operable in case of an emergency. Application to a fictitious attack against a critical infrastructure. Proc. 19th Int. Conf. on Harmonisation within Atmospheric Dispersion Modelling for Regulatory Purposes, Bruges, Belgium, 3-6 June 2019.

Armand, P., O. Oldrini, C. Duchenne and S. Perdriel, 2021: Topical 3D modelling and simulation of air dispersion hazards as a new paradigm to support emergency preparedness and response. *Env. Mod. & Soft.*, 143, 105129.

Baumann Stanzer, K. et al., 2015: Model evaluation case studies: Approach and results. COST Action ES1006.

Hanna, S. and J. Chang, 2012: Acceptance criteria for urban dispersion model evaluation. Meteorology and Atmospheric Physics, 116, 133–146.

Oldrini, O. and P. Armand, 2019: Validation and sensitivity study of the PMSS modelling system for puff releases in the Joint Urban 2003 field experiment. *Bound-Layer Meteorol*., 171 (3), 513-535.

Oldrini, O., P. Armand, C. Duchenne, C. Olry and G. Tinarelli, 2017: Description and preliminary validation of the PMSS fast response parallel atmospheric flow and dispersion solver in complex built-up areas. *Env. Fluid Mech.*, 17 (3), 1-18.

Oldrini, O., P. Armand, C. Duchenne and S. Perdriel, 2019: Parallelization performances of PMSS flow and dispersion modelling system over a huge urban area. *Atmosphere* 10 (7), 404.

Oldrini, O., P. Armand, C. Duchenne, S. Perdriel and M. Nibart, 2021a: Accelerated time and high-resolution 3D modeling of the flow and dispersion of noxious substances over a gigantic urban area – The EMERGENCIES project. *Atmosphere*, 12 (5), 640.

Oldrini, O., S. Perdriel, P. Armand and C. Duchenne, 2021b: High speed visualization of very large high-resolution simulations for air hazard transport and dispersion. *Atmosphere*, 12 (7), 920.

Tinarelli, G. et al., 2013: Review and validation of Micro-Spray, a Lagrangian particle model of turbulent dispersion. In Lagrangian Modelling of the Atmosphere, Geophysical Monograph, Vol. 200, 311-327.

Trini Castelli S. et al., 2016: Evaluation of local-scale models for accidental releases in built environments – Results of the modelling exercises in COST Action ES1006. In Air Pollution Modeling and its Application XXIV, Springer International Publishing Switzerland, 497-502.

Trini Castelli, S., P. Armand, G. Tinarelli, C. Duchenne and M. Nibart, 2018: Validation of a Lagrangian particle dispersion model with wind tunnel and field experiments in urban environment. *Atmos. Env.*, 193, 273-289.